A Pilot on the use of Stride Cadence for the Characterization of Walking Ability in Lower Limb Amputees

Ejay Nsugbe [a,*], Oluwarotimi Williams Samuel [b], Mojisola Grace Asogbon [c], and Jose Javier Reyes-Lagos [d]

[a] Nsugbe Research Labs, Swindon, UK; ennsugbe@yahoo.com
[b] School of Computing and Engineering, University of Derby, Derby, UK; o.samuel@derby.ac.uk
[c] Shenzhen Institute of Advanced Technology, Chinese Academy of Sciences, China; grace@siat.ac.cn
[d] School of Medicine, Autonomous University of Mexico State (UAEMéx), Toluca de Lerdo, Mexico; jjreyesl@uaemex.mx
* Correspondence: ennsugbe@yahoo.com

Abstract: Amputations are a prominent affliction that occur worldwide, with causes ranging from congenital, disease-based, or external reasons such as trauma. Prosthesis provides the closest alternative functional replacement to the loss of a limb. Before any form of rehabilitation support can be offered to amputee patients, an assessment of their degree and level of mobility first needs to be evaluated using the K-level grading system. The typical means towards the assigning of a K-level grading is through qualitative methods, which have been criticized for being subjective and, at times, imprecise. As a means towards remedying this shortcoming, we investigated the prospect of utilizing data from wearable sensors for analyzing the stride pattern and cadence of various subjects towards the quantitative inference of a K-level. This was accomplished using data from accelerometers, alongside advanced signal processing and machine learning models, towards the quantitative identification and differentiation of the various K-levels of amputees of varied levels of mobility. The experimental results showed that this aim could be accomplished under the circumstance investigated and the models applied as part of this research. Additional analysis was also done on the use of data from accelerometers towards the differentiation between amputated and non-amputated subjects, which showed that the cohorts could be classified and differentiated using purely accelerometer data and the accompanying postprocessing methods.

Keywords: Lower limb; Signal processing; Machine learning; Artificial intelligence; LSDL; Prosthesis; Wearable sensors; Amputations; Biomechanics; Orthopedics

1. Introduction

Amputations are a global phenomenon that can occur due to a host of reasons which can be primarily summarized into three categories: traumas, diseases and multifarious reasons [1–5]. Traumatic amputations could occur due to accidents, burns or sports, for example. Diseases leading to amputations include diabetes, cancers, frostbite, blood infections and osteomyelitis [1–5]. Other reasons which could lead to amputations can include congenital manifestations and clinical negligence [1–5]. A structured visualization of various common causes of amputations can be seen in Figure 1.

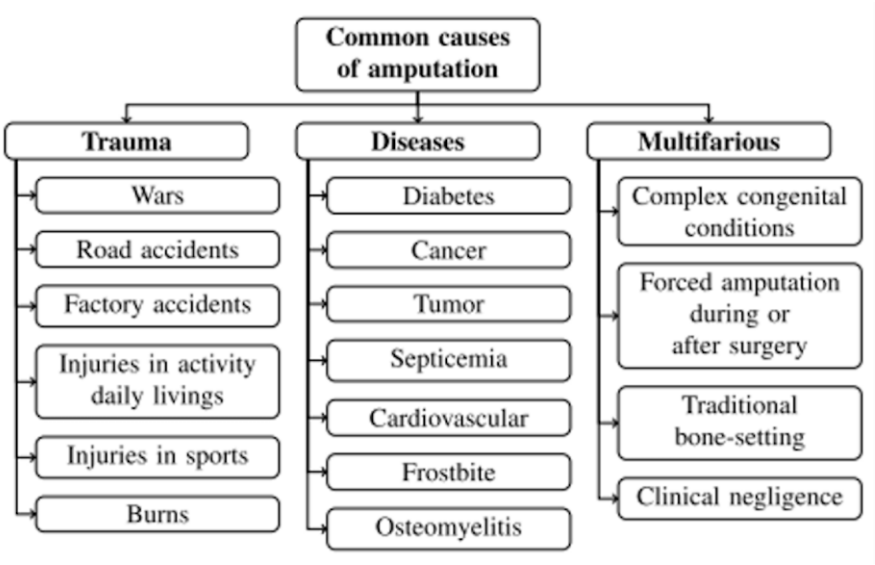

Figure 1. Various common causes of amputations [1].

A global amputation root cause analysis study, conducted on around 30,000 patients in various regions around the world, has helped showcase the leading causes of amputations within each region [6]. It can be inferred that the causes of amputations in certain regions can be linked to the characteristics of the region, i.e., poor socioeconomic status, wars and conflict, among others. A summary snapshot showing the results of the survey conducted over 15 years in many countries worldwide can be seen in Figure 2 [1,7–11].

Year	Country	# of Patients	Survey Period	Etiology (Study of causes i.e. trauma & diseases)
2005	Thailand	216	05 Years	Incidents and vascular diseases
2007	Nigeria	1642	15 Years	Trauma, tumor, diabetes, traditional bone-setting
2009	Korea	4258	24 Years	Trauma, peripheral vascular disease
2009	France	17552	01 Year	Bone disease, injury, neurological disease
2011	Australia	3400	01 Year	Trauma and diabetes
2012	Tanzania	162	02 Years	Trauma, diabetes
2012	Australia	186	01 Years	Diabetes, peripheral arterial disease, trauma
2012	Iran	624	09 Years	Trauma
2013	India	155	02 Years	Vascular diseases, trauma, and carcinoma
2013	Iran	160	05 Years	Trauma, vascular problems, and infection
2013	Iran	216	10 Years	Trauma
2015	New Zealand	892	07 Years	Diabetic type-2
2016	Sri Lanka	85	01 Year	Diabetes mellitus, vascular disease, septicemia
2016	Pakistan	123	03 Years	Trauma
2017	Bahrain	45	01 Year	Diabetes mellitus
2019	Nigeria	136	10 Years	Diabetes neuropathy
2019	Pakistan	5836	04 Years	Trauma and diabetes
2020	Ireland	172	09 Years	Non-traumatic (vascular)
2020	Cameroon	172	02 Years	Trauma
2021	Nigeria	93	05 Years	Peripheral vascular diseases
2021	South Africa	152	01 Year	Peripheral vascular diseases, diabetes mellitus

Figure 2. Results of a 15-year survey of lower limb amputation in various countries. The source table can be found in Asif *et al*. [1].

An annotated image of a skeletal view of the lower limbs can be seen in Figure 3, where it can be noted that each degree of limb loss has an associated technical terminology used to describe the condition.

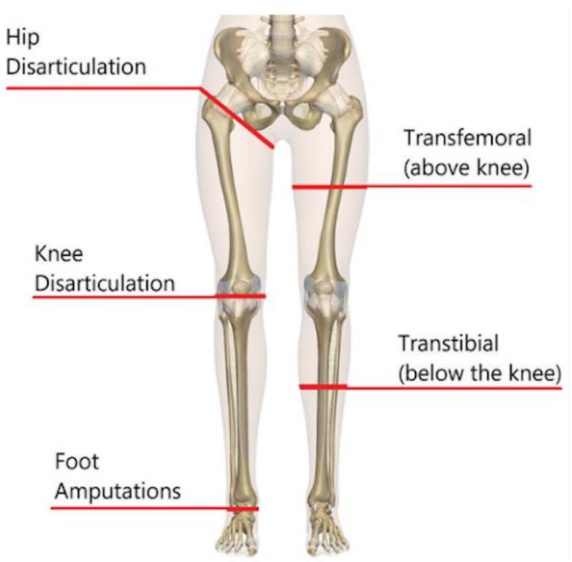

Figure 3. Skeletal view of the lower limbs with various levels of amputation [12].

Within the UK, estimates of the costs associated with lower limb amputations to the NHS span £10,000–15,000 per procedure, which accumulates to around £50–75 million per annum and accounts for 0.5% of the NHS' budget [13]. This figure rises when factors such as rehabilitation care and prosthesis support are added into the costing model [13].

In terms of functional replacements for the loss of a lower limb, prosthesis devices can be adopted by amputees. There are three categories of lower limb prosthesis: i) the passive, which has components of fluidic and mechanized configurations; ii) the active, which are driven by an electromechanical output; and iii) the semiactive, which embodies a hybrid between the aforementioned pair [1]. A hierarchical snapshot showing the various kinds of prosthesis, as well as their subcategories, can be seen in Figure 4.

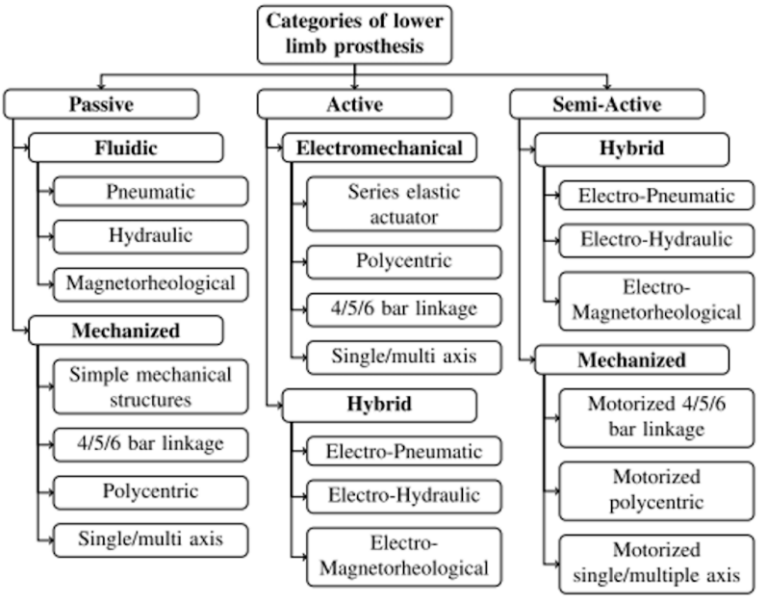

Figure 4. A hierarchical snapshot of the various kinds of prosthesis, along with subcategories [1].

There are currently 10 branded variants of lower limb prosthesis, which are embedded with various kinds of sensors, including inertial measurement units (IMUs), force resistance sensors, accelerometers and EMG sensors, to name a few [14–16]. These brands include: SACH foot, which is a clas-

sic variant with mostly mechanical components; Orion is a microprocessor-based, transfemoral prosthesis; Plie is fairly lightweight and allows for loading up to 125 kg; Genium is a microprocessor-based, passively driven hydraulic prosthesis with embedded IMUs; and Empower presents a variant of a bionic prosthesis which is tailored towards transtibial amputees who require functionality upstairs, and on ramps and hills [1,17–19]. Rheo Knee is based around a microprocessor magnetorheological system which is capable of a continuous adaptation to the various terrains that it is surrounded by; while Power Knee represents a kind of intelligent prosthesis for transfemoral amputees which aids the restoration of lost power in the muscles and the symmetry of movement patterns [1,17–19]. SmartIP is a semiactive prosthesis system powered through hydraulic, pneumatic and electrochemical power; whereas the PROPRIO FOOT is a semiactive transtibial prosthesis with an objective that is based around the replication of the human foot via a series of motorized ankle flexion systems [1,17–19]. Finally, C-Leg is a transfemoral prosthesis which has IMUs, strain gauges and knee angle sensors embedded within it [1].

Some of the control strategies adopted as part of the lower limb prosthesis include finite state, impedance, least square, dynamic programming, predictive control, and fuzzy logic [20–26]. All of these are tailored towards achieving various control objectives such as aiding natural movement, stability, and gait approximations [20–26]. As part of the estimation and identification problem in the control scheme, machine learning models have been adopted with the aims of achieving feats such as terrain trajectory planning, fall detection, terrain identification, gait detection, and stance phase detection [20–26].

Within the field of lower limb amputation, the K-level is a metric that is used to determine the level of disability of an amputated patient [27]. The scheme works with a rating of 0–4, where a lower figure indicates a lessened level of mobility [27]. The various ratings are described as follows [27]:

K-0: is indicative of a patient with limited mobility who requires support for basic movement activities, and the provision of a prosthesis would not enhance their overall quality of life.

K-1: this kind of patient would benefit from the use of prosthesis, which would allow for them to walk at a fixed speed or cadence.

K-2: this kind of patient has mobility to a degree with a prosthesis, which would allow for them to navigate their way through environmental barriers such as uneven surfaces and curbs.

K-3: a prosthesis for this type of patient allows for mobility at various cadences or multiple speeds, including for activities that supersede basic locomotion, i.e., exercise etc.

K-4: the patient is capable of an exceedingly high amount of mobility, and this level is typically indicative of amputee patients who are Paralympians and/or athletes.

The conventional means towards the assignment of K-levels typically involves the holistic assessment of patient history, along with the state of the residual limb and the psychological condition of the patient, all of which are subjectively evaluated to yield a final K-level value [28–36]. These methods have been criticized considerably due to their subjective nature, and of course, occasionally being opinion-based [28–36]. Thus, there has been a growing desire for an alternative means towards the assignment of distinct K-level values based on gait and walking performance characteristics over the course of daily life [28–36]. However, significant work needs to be acknowledged which has been done by a group of authors who have adopted a set of biomechanical diagnostic devices for evaluating key mobility factors such as hip strength and mobility, as well as overall balance [37–42].

The steady uprise of wearable technologies has made it possible to have, in a sense, forms of mobile health monitoring schemes, which in this case can help support the monitoring of the mobility level of amputees [36]. These wearable technologies are primarily accelerometers and pedometers [36]. Using this approach, previous work has shown that the average amputee takes less than the recommended 10,000 steps per day [36,43]. More specifically, cadence and walking speed have been said to provide key information that can be related back to K-levels, and can be recorded inexpensively [36,43]. Prior related work has estimated the cadence rhythm using Weibull scale statistical parameters, from which it was deduced that smaller scale parameters were linked with a lower cadence rate, and so on, but relied on a continuous walking pattern [44]. The availability of wearable sensors has shown recorded uncertainty metrics under 0.10% [36].

In this study, we utilize the information from wearable sensors to monitor the cadence of various lower limb amputees towards a more quantitative method of assigning the K-level of an amputee. As part of this, and due to the information present alongside the accompanying data, we also look to investigate the extent to which an amputee vs a nonamputee could be differentiated solely based on their cadence. Furthermore, we conduct an auxiliary study to investigate whether there are distinct characteristics in the stride cadence of amputees who were amputated for different reasons, and thus have a varied perception of a phantom limb and a unique cadence rhythm. We aim to do all of this with the aid of advanced signal processing and machine learning models.

In terms of advanced signal processing, multiresolution and signal decomposition methods are chiefly used towards the separation of a signal into component parts in an attempt to minimize uncertainty and boost the overall quality of a signal [45–47]. The related literature includes the linear series decomposition learner (LSDL) and deep wavelet scattering (DWS) [48,49]. The LSDL represents a metaheuristic format, underpinned by a set of heuristics towards a continued systematic separation of a signal in subcomponents, with the knowledge that an optimal region within the signal would carry the greatest information quality and relatively less uncertainty [49,50]. The LSDL has proven to be useful in case studies involving nonlinear physiological signals, where it has been noted that the inclusion of the LSDL as a preprocessing mechanism prior to modelling activities has boosted the prediction accuracy within the case study itself [49,50].

On the other hand, the DWS represents a unique signal decomposition method which is embedded upon a merger between the wavelet transform and a deep learning architecture, i.e., a convolutional neural network, thus rendering aspects of its architecture to be black box based [48,51]. In addition to being a signal decomposition tool, the DWS also serves as a means towards (unsupervised) feature extraction, where its features are not interpretable due to its deep learning architecture [52]. The DWS represents a growing method that is beginning to be favored in the area of nonlinear signal processing since it also offers a feature extraction prowess, therein negating the need for expert knowledge in the context of feature extraction of the signal.

Machine learning represents the underpinning AI methods that are typically employed in pattern recognition exercises as a means towards creating a form of classification between various classes of data [53,54]. Machine learning models are broad and numerous, while a range of these models have seen a fluent application within rehabilitation and a multitude of other aspects of clinical medicine [53,54].

In this paper, we utilize accelerometer recorded cadence data from the feet of amputee and nonamputee subjects towards reaching the following contributions:

- The use of the cadence sequence from the accelerometer for the differentiation between amputee vs nonamputee patients.
- The differentiation of the mobility extent/K-level of various amputees using strictly the accelerometer data.
- An exploratory exercise to investigate whether the cadence data of subjects who have been amputated for different reasons—and thus experience varied phantom sensations—result in a difference in accelerometer data. This could lead towards the differentiation between the two classes of amputee patients.

From these, it is hypothesized that a deeper scientific understanding of the kind of biomechanical information that can be inferred from accelerometry datasets on lower limb amputees would be established.

2. Dataset

The dataset used for this study is taken from Kim *et al*. [36], where a mixture of amputated and nonamputated individuals were recruited at the University of Michigan Orthotics and Prosthetics Center. All of the chosen participants had to be over 18, and the amputees needed to have been using a prosthesis for around 6 months and be able to walk unaided. The amputees recruited as part of the study had a K-level range of around K2–K4, with all amputees ensuring that they had no neurological

diseases prior to being recruited. Informed consent was provided by both groups of participants, which was approved by the University of Michigan Institutional Review Board (HUM00096819) [36].

All subjects were directed to walk at a comfortable pace with both the ActiGraph GT9X Link and a Global Positioning System over the duration of the acquisition. The activity monitors were attached to the foot of each subject, as seen in Figure 5, where the sampling rate of the sensor used was 100 Hz.

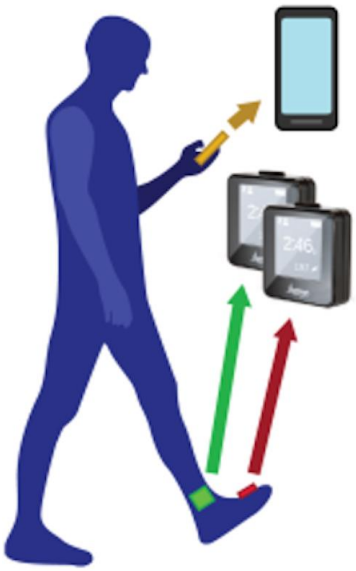

Figure 5. An image showing the accelerometer and IMU attached to a subject's foot, and a geographical tracking system in the form of a mobile phone (note that only the accelerometer data was utilized as part of the study) [36].

Figure 6 shows a breakdown of the various subjects whose data was recorded as part of the acquisition. Here, it can be seen that the majority of the subjects were unilateral transtibial amputees who were amputated for a range of reasons; namely, trauma, dysvascular and congenital. A total of 28 subject datasets were utilized as part of the study, where 14 of which were the nonamputees and the remaining 14 were amputees with ID numbers ranging from 1–15, since ID 03 amputee produced an error during the downloading process.

ID	Sex	Age	K-level	Level of amp	Cause	ACC (full days)	Total IMU strides[a]	IMU strides w/GPS[b]	Season	Sex	Age	ACC (full days)	Total IMU strides[a]	IMU strides w/GPS[b]	Season
01	M	52	3	UTT	trauma	12	25900	3450	Sp	M	29	14	28700	27600	W
02	F	43	2	TT+TF	vasc	12	2650	1830	W	M	26	14	8260	8260	W
03	M	20	3	UTF	cong	11	13700	11400	Sp	F	39	11	26200	25800	W
04	M	71	3	UTT	vasc	14	3200	3200	S	M	24	14	35400	30100	W
05	M	39	3	UTT	trauma	13	12000	11800	S	M	58	17	50100	41800	W
06	M	57	3	UTT	vasc	13	6600	4630	S	M	49	23	82600	36700	Sp
07	M	62	3	UTT	trauma	31	11000	8030	F	M	64	15	16600	15100	Sp
08	M	53	3	UTT	vasc	13	3050	3000	W	M	22	15	23200	19900	Sp
09	M	65	3	UTT	vasc	14	2500	1900	Sp	M	61	19	50400	45100	Sp
10	M	40	3	UTT	trauma	12	2270	2270	F	M	50	22	47700	45600	Sp
11	M	30	3	UTT	trauma	13	1720	1640	F	M	40	14	35400	35300	S
12	M	65	3	UTT	trauma	30	19400	18900	Sp	M	51	9	34700	32600	S
13	M	55	3	UTT	trauma	13	12500	12000	F	M	63	16	39600	32200	S
14	M	27	4	UTT	trauma	3	2220	773	F	M	43	13	29000	28000	S
15	M	54	4	UTT	trauma	19	11200	11100	W						
16	M	45	3	UTT	trauma	10	17600	17600	Sp						
17	F	37	2	UTT	vasc	15	827	752	S						
Mean		47.9				14.6	8710	6720			44.2	15.4	36300	30300	
(SD)		(14.5)				(6.75)	(7440)	(5960)			(14.8)	(3.84)	(18000)	(10800)	

List of abbreviations: amp: amputation, U: unilateral, TT: transtibial, TF: transfemoral, vasc: dysvascular, cong: congenital, Sp: Spring, S: Summer, F: Fall, W: Winter

Figure 6. Breakdown of the various subjects whose data was recorded as part of the acquisition. The source table can be found in Kim *et al*. [36].

From each subject, 20,000 samples x 3-axes from the accelerometer were used towards conducting the signal processing and machine learning exercise, resulting in 60,000 samples per subject. A visualization of the accelerometer signal from a sample segment of an amputee vs nonamputee can be seen in Figure 7.

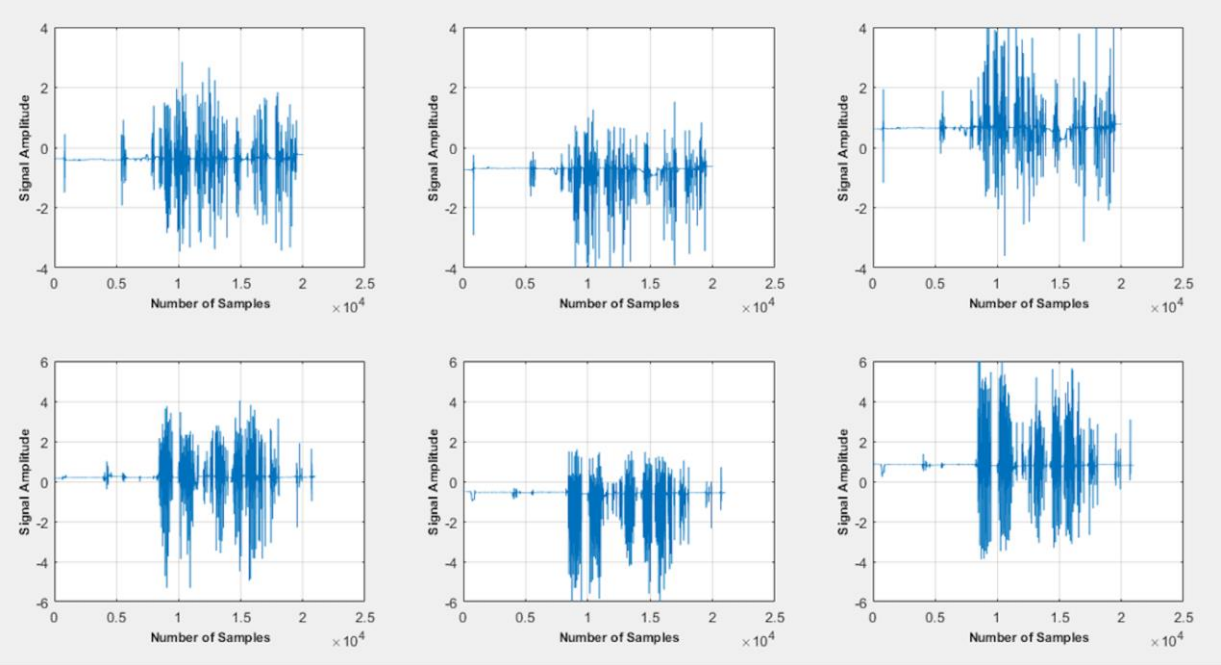

Figure 7. From left, the top three graphs correspond to the X, Y and Z axes of the accelerometer for the amputated subject, while the bottom three graphs correspond to the X, Y and Z axes of the accelerometer for the nonamputated subject.

When comparing the sets of graphs, it can be seen that there is a greater number of strides per interval and per unit time for the nonamputated subject than there is for the amputated patient. This elegantly reflects the mobility differences between the two cohorts by the level of dynamic activity in the timeframe visualized in the plots.

Methods and Approach (3–5)

3. Signal Decomposition Methods

Signal decomposition methods are based around a methodical separation of the signal into component parts in order to minimize noise, interferences and uncertainty, while boosting the overall signal quality. Two candidate methods were utilized for the signal decompositions in this work, namely, the metaheuristically driven LSDL and the deep learning based DWS. These two methods are described in sections 3.1 and 3.2.

3.1. LSDL

The LSDL represents the use of metaheuristic reasoning for the systematic decomposition of a candidate signal into component parts, with the use of a set of defined heuristics alongside a candidate basis function with an embedded cost function capable of assessing the quality of each candidate decomposition [49,50,53–57]. The inception case study for the LSDL was for source separation of a heterogenous powder mixture from structural borne acoustic emission waves for the inference of the particle size distribution [58]. During this study it was seen that the LSDL has unique capabilities towards the steady decomposition of nonlinear and stochastic signals, and when benchmarked with the classical wavelet transform the LSDL was seen to surpass its performance.

Due to this feat, the LSDL has seen applications in wider areas outside of its inceptive case study, namely, in aspects of clinical medicine where mostly nonlinear physiological signals are acquired.

The application of the LSDL has spanned areas such as rehabilitation, preterm pregnancy, surgical anesthesia and psychiatric medicine [54,57,59,60]. The LSDL has found a pivotal base being utilized as a preprocessing tool for the various sources of physiological signals prior to modelling and the associated prediction exercises.

The LSDL contains an embedded cost function which is capable of assessing the "goodness" and quality of information from the subsequent decomposed time-series, where the embedded cost function is in the form of the normalized Euclidean distance metric. The normalization act serves to null out the limitation of a scale variance typically associated with the Euclidean distance.

A mathematical formulation of the LSDL, alongside its supporting heuristics and underpinning reasoning, can be seen in Nsugbe *et al*. [50].

3.1.1. Optimal Threshold Search

As per the sequence of the LSDL, two candidate signals were selected from different classes and utilized as part of the optimization process, which saw a multitude of decompositions using the preformulated tuning heuristics. Each candidate decomposition was assessed using the embedded cost function, the results of which can be seen below in Table 1.

Table 1. Results of candidate decomposition for the LSDL.

	1st Iteration	**2nd Iteration**	**3rd Iteration**
Upper Threshold	2.099	2.014	n/a
Lower Threshold	2.005	2.007	2.071

For each figure displayed in Table 1, the same decomposition region for the two classes being considered were compared, from which a final figure was obtained, as seen in Table 1. It can be noted that a total of 12 slices of decomposed signals were considered to assemble the list of figures, where the optimization objective here is the selection of the region with the highest performance index. The region with this value is subsequently regarded as the optimal threshold region, alongside its associated decomposition threshold parameters.

The results show that the optimal threshold region resides within the 1st iteration of the upper threshold, which largely reflects that the upper amplitude region and the lower frequency aspects of the signal contain the key information within the signal, which is necessary for the modelling of the various signals.

3.2. DWS

Convolutional neural networks (CNNs) are a form of unsupervised feature learning method where multiscale features of a training sample are learned and acquired [61–63]. The DWS combines properties of both the CNN and the classical wavelet transform towards producing multiscale decompositions and learned features from candidate samples [61–63]. It is said that the DWS possesses the following key properties associated with its main stages: convolution with a mother wavelet; nonlinearity due to a modulus; which is succeeded by a filtering and averaging act using wavelet low pass filters, which forms an analogue for pooling [61–63].

The joint property of the DWS makes it a form of both a signal decomposition mechanism and an unsupervised feature extraction tool. It is said that the acquired multiscale features from the DWS are of low variance, which are continuous and also robust to translations [61–63]. The key difference between the DWS's CNN architecture and a standard CNN is the use of predefined configurations, i.e., wavelet and scaling filters, instead of an iterative learning sequence from data. In a way this poses as a strength, as fewer samples are required to reach a computational optimum [61–63].

Some of the key similarities between both architectures include contractions at a multiscale and linearization of hierarchical symmetries, as well as sparse representations. A block diagram series depicting the various stages associated with the DWS can be seen in Figure 8 [61–63].

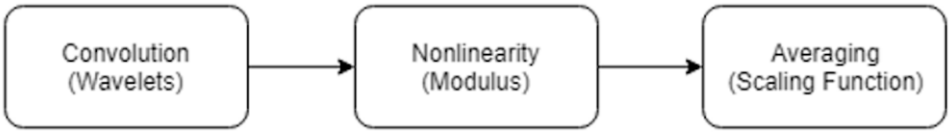

Figure 8. Stages of the DWS [61].

In terms of the mathematical formalism of the method, Liu *et al*. [64] proposed a signal $f(t)$ being analysed by a low pass filter $\emptyset$, and a wavelet function Ψ spanning different frequencies for a low pass filter $\emptyset_J(t)$, which provides a form of specialized translation invariance f with a specified scale T. A family of wavelet indices possessing an octavian-based resolution Q_k is denoted as $\wedge_k$, while the multiscale high pass filter banks $\{\Psi_{jk}\}_{jk\in\wedge_k}$ are assembled with a dilation of the wavelet Ψ [61–63].

In the DWS, a wavelet scattering network is put into play with the use of a deep CNN which, as anticipated, performs a convolutional act via classical wavelets, a nonlinear modulus, and an averaging scaling function [61–63]. For the convolution part, $S_0 f(t) = f * \emptyset_J(t)$ (for which S_0 is the zero-order scattering coefficients) generates locally translation invariant features of f where, despite yielding a degree of information loss at the higher frequencies, an information recovery act is initiated via a wavelet modulus transform $|W_1|$, as expressed in Equation 1 [61–63]:

$$|W_1|f = \{S_0 f(t), |f * \Psi_{j1}(t)|\}_{j1\in\wedge_1} \quad (1)$$

In a hierarchical manner, the first order scattering coefficients can be obtained with the averaging of the modulus coefficients with $\emptyset_J(t)$, as described in Equation 2 [61–63]:

$$S_1 f(t) = \{|f * \Psi_{j1}(t)| * \emptyset_J(t)\}_{j1\in\wedge_1} \quad (2)$$

Once again, the sequence to recover any information lost during the averaging process, with respect to the notion that $S_1 f(t)$, can be viewed as the low frequency component of $|f * \Psi_{j1}|$, while the wavelet modulus of the high frequency can be expressed as Equation 3 [61–63]:

$$|W_2||f * \Psi_{j1}| = \{S_1 f(t), ||f * \Psi_{j1}| * \Psi_{j2}(t)|\}_{j2\in\wedge_2} \quad (3)$$

Which subsequently gives rise to the second order coefficients in Equation 4:

$$S_2 f(t) = \{||f * \Psi_{j1}| * \Psi_{j2}| * \emptyset_J(t)\}_{j2\in\wedge_2} \; i = 1,2. \quad (4)$$

A continuous iteration of the defined process yields the wavelet modulus convolutions shown in Equation 5:

$$U_m f(t) = \{||f * \Psi_{j1}| * \ldots..| * \Psi_{jm}|\}_{j1\in\wedge_1}, i = 1,2, \ldots m. \quad (5)$$

Where U_m is an mth order modulus. The procedure towards obtaining the mth order scattering coefficients, $U_m f(t)$ with $\emptyset_J$, can be seen as follows in Equation 6:

$$S_m f(t) = \{||f * \Psi_{j1}| * \ldots..| * \Psi_{jm}| * \emptyset_J(t)\}_{j1\in\wedge_1}, i = 1,2, \ldots m \quad (6)$$

This approach is utilized towards obtaining the final scatter matrix $Sf(t) = \{S_m f(t)\}_{0\le m\le l}$, which merges all the scattering coefficients from all orders as a means of characterizing an input signal for l decompositions. A hierarchical tree visualization of the method, can be seen in Figure 9.

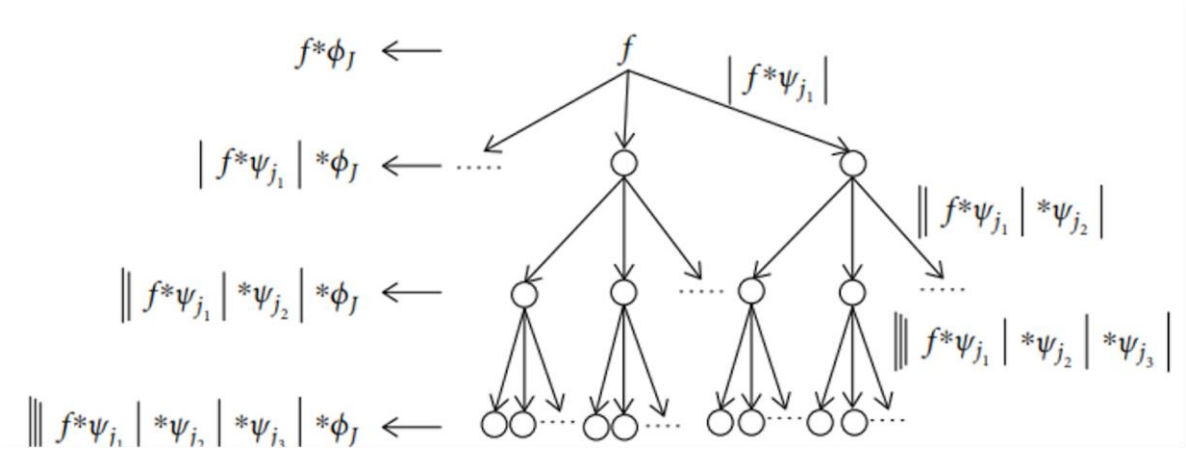

Figure 9. A tree-based visualization of the scattering decomposition network, where the output features are not solely from the final layer, as per the standard CNN, but a from combination of all preceding layers [64].

As the energy content of the scattering coefficients saturates with an increasing number of layers, it has been noted that the bulk of the energy in the signal is hosted within the first two layers. Due to this, only the information of the first two layers of the network was utilized for the analysis in this work. Supporting parameters utilized as part of the wavelet scattering decomposition involved the use of the Gabor wavelet as the mother wavelet, with the scale invariance set to 1, based on the results from previous work [57]. The other default parameters were 8 wavelets per octave in the first filter bank, in addition to 1 wavelet per octave in the second filter bank [57].

4. Feature Extraction

A range of features were extracted from the accelerometer signals, which were applied in a prior study for the characterization of nonlinear signals [65]. This group of features comprises the linear statistics all the way towards chaos-based features, which are expected to contribute towards an effective characterization and modelling of the candidate signal [65]. The range of features were adopted from Nsugbe *et al*. [65], which readers should consult for more details on the feature set itself. For all features a threshold of 1 μv was used, while for the entropy features, 0 and 0.2 values were chosen for m and r respectively.

5. Machine Learning

- **Decision Tree (DT):** is a grey box model driven off Boolean logic, and partitions data into various groups in a hierarchical fashion [66]. The decision making scheme of these models is largely interpretable, hence they have an air of transparency associated with their decision making [66].
- **Discriminant Analysis:** this machine learning model is embedded upon statistical reasoning where, at first, a lower dimensional projection of the dataset is performed, and succeeded by a placement of the various class boundaries [67]. In this work, both the linear and quadratic class boundaries were utilized in various capacities, hence the linear discriminant analysis (LDA) and quadratic discriminant analysis (QDA).
- **Logistic Regression (LR):** represents another statistically driven classification framework which outputs classification scores in a range that spans 0–1 [68]. The approach utilizes a sigmoid towards the robustified distinguishing between classes when contrasted against its linear regression counterpart [68].
- **K-Nearest Neighbor (KNN):** is a kind of nonparametric classification model which is based upon a majority voting scheme towards assigning samples to different classes [69]. K was selected as 1 in this work, in the interest of computational efficiency, while the Euclidean distance was used as the means of calculating the distance between data classes [69].

The MATLAB classification learner application was utilized for all the machine learning model build exercises, where the hyperparameters associated with each model were tuned automatically

and iteratively as part of the build process. The k-fold cross validation scheme was used for validating the final models, where k was chosen to be 10.

6. Results

6.1. Differentiation of Amputees vs Nonamputees via Cadence

The results in Table 2 show the various classification accuracies for the differentiation between amputees vs nonamputees, based purely from the cadence pattern obtained from their accelerometer datasets. For the direct use of the raw signal, the best model performance was seen to be the LDA, with a classification accuracy of 61%. A substantial performance increase was seen in the case of the LSDL, where the best accuracy was obtained at 96% for the LR model, once again showcasing the power of the LSDL as a preprocessing tool for time-series signals. For the DWS, the best classification accuracy was 85%, this time for the KNN model. Contrasting the performance metrics obtained for all three methods, it can be seen that the LSDL boasts the best performance across the board, emphasizing its prowess in reducing the overall uncertainty within a time-series signal. However, it needs to be mentioned that there is no one-size-fits-all best classification model, irrespective of the method used. Rather, it can be noted that the optimal classification model varied across all methods, spanning the LDA, LR, and KNN.

Table 2. Classification accuracies for differentiation between amputees vs nonamputees.

Model	Raw Signal (%)	LSDL (%)	DWS (%)
Tree	59	60	69
LDA	61	94	58
QDA	n/a	n/a	57
LR	61	96	59
KNN	64	76	85

Figure 10 shows the principal component analysis (PCA) projection for the various tables presented in this subsection, from which it can be seen that the best projection and maximal cluster separation was seen to occur for the LSDL. Once again, this showcases the power of the LSDL as a preprocessing tool prior to subsequent signal modelling. It can be noted that the number of samples for the DWS is increased relative to the other two methods, due to the multiscale dilation properties of the DWS.

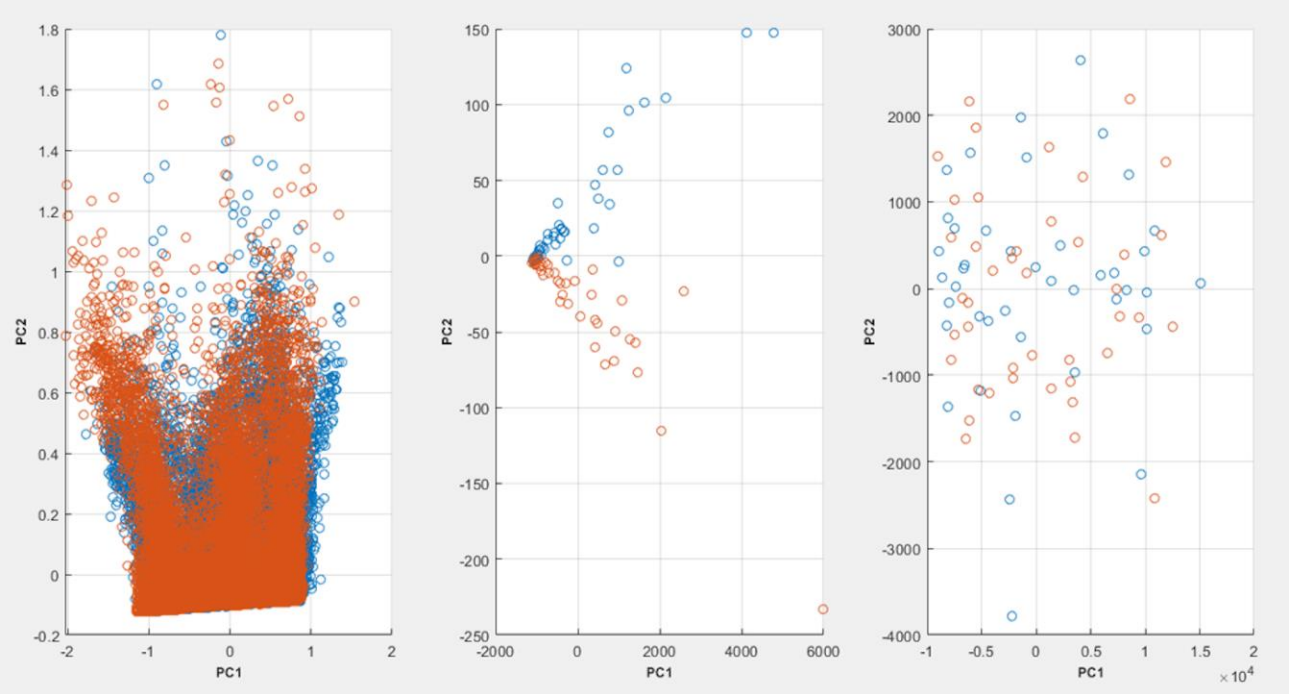

Figure 10. PCA plot with 98% variability explained. Left: DWS; Middle: LSDL; Right: Raw signal.

6.2. Prediction of K-level

For this case study, the DWS was used as the analytical method. This was due to the optimal LSDL threshold not finding any signal peaks for some of the selected amputee dataset, thus returning zeros in certain cases. A total of six amputee patients' datasets were used, of which there were two patients from the K-levels 2–4. This case study was based around the investigation to see if the K-levels can be inferred solely from the accelerometer dataset, and therein be used as a means towards assigning the K-level in future scenarios.

The results from the K-level prediction exercise can be seen in Table 3, from which it can be noted that the best performance metric was for the LR model, which boasted an accuracy of 82%. This indicates a generally high and reliable performance metric, suggesting that the proposed method could be leveraged towards the assignment of K-level based on a combination of accelerometer data and the DWS postprocessing.

Table 3. Classification accuracy of the DWS from the accelerometer dataset.

Model	Classification Accuracy (%)
Tree	72
LDA	55
QDA	48
LR	82
KNN	n/a

However, it should be mentioned that the sample size used as part of this case study was rather small and constrained, but the multiscale contraction property of the DWS helped to serve as a sample population characteristic to broaden the sample size. Nevertheless, further work would need to be done with a broader sample size in order to investigate this notion more thoroughly.

6.3. Cause of Amputation Differentiation

As per the Penfield homunculus, the different body parts requiring a sense of motor activity have a unique mapping across the cortex in the human brain [70–72]. Postamputation, the neurological mapping of that particular limb remains in the homunculus, as well as the afferent and efferent nerve pathways in a closed loop within the brain [70–72]. This accounts for a plausible explanation behind so-called phantom limb sensations, or the ghosts of departed limbs [70–72].

It is presumed that different kinds of underpinning reasons behind amputations could contribute towards a unique kind of phantom sensation, post-limb-loss. This could manifest itself further by resulting in varied stride biomechanics and cadence rhythm in the subamputee population, and can be captured with an accelerometer.

For this case study, the DWS was used once again, and two patients' data was used from two groups: amputation due to, i) trauma; and ii) a dysvascular disease, which thus amounted to four datasets in total. The results can be seen in Table 4, where the KNN model provided the best classification accuracy. In a sense, this provides some evidence that the phantom motions do indeed influence the subsequent stride and cadence patterns of the amputees. As with the prior case study in section 6.2, a much bigger study would need to be done in order to thoroughly investigate the consistency of this.

Table 4. Classification accuracy of the DWS for two types of amputation (trauma and dysvascular disease).

Model	Classification Accuracy (%)
Tree	83
LDA	68
QDA	70
LR	69
KNN	88

7. Conclusion and Future Work

Amputations are widespread and occur around the world for a multitude of reasons, including trauma and disease. Epidemiological studies have shown that the drivers behind amputations can be linked and traced to the socioeconomic region and political agenda of a country. Lower limb prostheses serve as a functional replacement for various degrees of lower limb losses, which are categorized as passive, active, and a semiactive intermediary. Not long after amputation, the mobility extent of an amputee is evaluated using a derived K-level scheme which spans from 0–4, with a higher figure indicating a greater level of mobility. The typical means of assigning K-levels include a qualitative assessment of both the mobility patterns and the nature of the residual tissue of the amputated stump. Results have indicated that there is a considerable amount of subjectivity in the assignment of these various K-levels, which warrants the desire for a more quantitative approach towards the assignment of these values.

In this study, we utilized the accelerometer dataset from both amputated and nonamputated subjects to investigate whether it is possible to differentiate between them purely from their stride rhythm and cadence, while also identifying the K-levels of amputees. The results showed that the subjects can be differentiated between with a high degree of accuracy while utilizing the LSDL preprocessing algorithm. For the K-level identification work, it was seen that the K-levels could be identified using purely accelerometer data from stride patterns with the use of the DWS. Hence, this forms initial evidence supporting potential application in a clinical setting towards a more accurate means of assessing degrees of mobility in amputated patients.

Subsequent work in this area could involve the collection of a broader range of data from amputees with a full range of K-levels in order to further, and more robustly, test and investigate this notion and developed model.

Author Contributions: All authors contributed equally to the manuscript

Institutional Review Board Statement: The study received ethical approval from the relevant body, as is mentioned within the manuscript.

Informed Consent Statement: Informed consent was obtained from all subjects involved in the study.

Data Availability Statement: Data is available from a cited repository within the manuscript

Acknowledgments: The authors would also like to thank Brian Kerr from Kerr Editing for proofreading this manuscript.

Funding: This research did not receive any specific grant from funding agencies in the public, commercial, or not-for-profit sectors.

Conflicts of Interest: The authors declare no conflict of interest.

References

[1] Asif M, Tiwana MI, Khan US, Qureshi WS, Iqbal J, Rashid N, et al. Advancements, Trends and Future Prospects of Lower Limb Prosthesis. IEEE Access 2021;9:85956–77. https://doi.org/10.1109/ACCESS.2021.3086807.

[2] Esquenazi A, Kwasniewski M. Lower Limb Amputations: Epidemiology and Assessment. PM&R KnowledgeNow 2017. https://now.aapmr.org/lower-limb-amputations-epidemiology-and-assessment/ (accessed March 23, 2023).

[3] Waters RL, Perry J, Antonelli D, Hislop H. Energy cost of walking of amputees: the influence of level of amputation. J Bone Joint Surg Am 1976;58:42–6.

[4] Hak L, van Dieën JH, van der Wurff P, Prins MR, Mert A, Beek PJ, et al. Walking in an unstable environment: strategies used by transtibial amputees to prevent falling during gait. Arch Phys Med Rehabil 2013;94:2186–93. https://doi.org/10.1016/j.apmr.2013.07.020.

[5] Paysant J, Beyaert C, Datié A-M, Martinet N, André J-M. Influence of terrain on metabolic and temporal gait characteristics of unilateral transtibial amputees. J Rehabil Res Dev 2006;43:153–60.

[6] Moxey PW, Gogalniceanu P, Hinchliffe RJ, Loftus IM, Jones KJ, Thompson MM, et al. Lower extremity amputations--a review of global variability in incidence. Diabet Med 2011;28:1144–53. https://doi.org/10.1111/j.1464-5491.2011.03279.x.

[7] Settakorn J, Rangdaeng S, Arpornchayanon O, Lekawanvijit S, Bhoopat L, Attia J. Why were limbs amputated? An evaluation of 216 surgical specimens from Chiang Mai University Hospital, Thailand. Arch Orthop Trauma Surg 2005;125:701–5. https://doi.org/10.1007/s00402-005-0060-y.

[8] Fosse S, Hartemann-Heurtier A, Jacqueminet S, Ha Van G, Grimaldi A, Fagot-Campagna A. Incidence and characteristics of lower limb amputations in people with diabetes. Diabet Med 2009;26:391–6. https://doi.org/10.1111/j.1464-5491.2009.02698.x.

[9] Lazzarini PA, O'Rourke SR, Russell AW, Clark D, Kuys SS. What are the key conditions associated with lower limb amputations in a major Australian teaching hospital? J Foot Ankle Res 2012;5:12. https://doi.org/10.1186/1757-1146-5-12.

[10] Sabzi Sarvestani A, Taheri Azam A. Amputation: a ten-year survey. Trauma Mon 2013;18:126–9. https://doi.org/10.5812/traumamon.11693.

[11] Rani A, Hamza M, Asma A, Tariq I, Osama B. Major lower limb amputation: causes, characteristics and complications. Bahrain Medical Bulletin 2017;39:159–61.

[12] Hussain S, Shams S, Jawaid Khan S. Impact of Medical Advancement: Prostheses. In: Wang L, Yu L, editors. Computer Architecture in Industrial, Biomechanical and Biomedical Engineering, IntechOpen; 2019. https://doi.org/10.5772/intechopen.86602.

[13] Moxey PW, Hofman D, Hinchliffe RJ, Jones K, Thompson MM, Holt PJE. Epidemiological study of lower limb amputation in England between 2003 and 2008. Br J Surg 2010;97:1348–53. https://doi.org/10.1002/bjs.7092.

[14] Goh JC, Solomonidis SE, Spence WD, Paul JP. Biomechanical evaluation of SACH and uniaxial feet. Prosthet Orthot Int 1984;8:147–54. https://doi.org/10.3109/03093648409146077.

[15] Rihs D, Polizzi I. Prosthetic Foot Design. StudylibNet 2001. https://studylib.net/doc/18100946/prosthetic-foot-design (accessed March 23, 2023).

[16] Orion3. Orion3 n.d. https://www.blatchfordmobility.com/en-us/products/knees/orion3/ (accessed March 23, 2023).

[17] Laschowski B, Andrysek J. Electromechanical Design of Robotic Transfemoral Prostheses. Volume 5A: 42nd Mechanisms and Robotics Conference, Quebec City, Quebec, Canada: American Society of Mechanical Engineers; 2018, p. V05AT07A054. https://doi.org/10.1115/DETC2018-85234.

[18] Zahedi S, Sykes A, Lang S, Cullington I. Adaptive prosthesis – a new concept in prosthetic knee control. Robotica 2005;23:337–44. https://doi.org/10.1017/S0263574704001365.

[19] PROPRIO FOOT® — Because the world isn't flat. Ossur.com. OssurCom n.d. https://www.ossur.com/en-us/prosthetics/feet/proprio-foot (accessed March 23, 2023).

[20] Yuan K, Zhu J, Wang Q, Wang L. Finite-State Control of Powered Below-Knee Prosthesis with Ankle and Toe. IFAC Proceedings Volumes 2011;44:2865–70. https://doi.org/10.3182/20110828-6-IT-1002.03064.

[21] Au SK, Herr H, Weber J, Martinez-Villalpando EC. Powered Ankle-Foot Prosthesis for the Improvement of Amputee Ambulation. 2007 29th Annual International Conference of the IEEE Engineering in Medicine and Biology Society, 2007, p. 3020–6. https://doi.org/10.1109/IEMBS.2007.4352965.

[22] Lawson BE, Ruhe B, Shultz A, Goldfarb M. A powered prosthetic intervention for bilateral transfemoral amputees. IEEE Trans Biomed Eng 2015;62:1042–50. https://doi.org/10.1109/TBME.2014.2334616.

[23] Fey NP, Simon AM, Young AJ, Hargrove LJ. Controlling Knee Swing Initiation and Ankle Plantarflexion With an Active Prosthesis on Level and Inclined Surfaces at Variable Walking Speeds. IEEE J Transl Eng Health Med 2014;2:2100412. https://doi.org/10.1109/JTEHM.2014.2343228.

[24] Gregg RD, Lenzi T, Hargrove LJ, Sensinger JW. Virtual Constraint Control of a Powered Prosthetic Leg: From Simulation to Experiments with Transfemoral Amputees. IEEE Trans Robot 2014;30:1455–71. https://doi.org/10.1109/TRO.2014.2361937.

[25] Kumar NA, Hong W, Hur P. Impedance Control of a Transfemoral Prosthesis using Continuously Varying Ankle Impedances and Multiple Equilibria 2019. https://doi.org/10.48550/arXiv.1909.09299.

[26] Yuan K, Wang Q, Zhu J, Wang L. A Hierarchical Control Scheme for Smooth Transitions between Level Ground and Ramps with a Robotic Transtibial Prosthesis. IFAC Proceedings Volumes 2014;47:3527–32. https://doi.org/10.3182/20140824-6-ZA-1003.02667.

[27] Bissontz J. What are K-Levels? | Innovative Prosthetic Solutions, Inc. What Are K-Levels? 2020. https://www.ipsprosthetics.com/what-are-k-levels/ (accessed March 23, 2023).

[28] Gailey RS, Roach KE, Applegate EB, Cho B, Cunniffe B, Licht S, et al. The Amputee Mobility Predictor: An instrument to assess determinants of the lower-limb amputee's ability to ambulate. Archives of Physical Medicine and Rehabilitation 2002;83:613–27. https://doi.org/10.1053/apmr.2002.32309.

[29] HCFA Common Procedure Coding System (HCPCS) 2001. Documentation. Springfield, VA, USA: U.S. Department of Commerce; 2000.

[30] Kaluf B. Evaluation of Mobility in Persons with Limb Loss Using the Amputee Mobility Predictor and the Prosthesis Evaluation Questionnaire Mobility Subscale: A Six-Month Retrospective Chart Review. JPO Journal of Prosthetics and Orthotics 2014;26:70–6. https://doi.org/10.1097/JPO.0000000000000020.

[31] Corrigan R, McBurney H. Community ambulation: Environmental impacts and assessment inadequacies. Disability and Rehabilitation 2008;30:1411–9. https://doi.org/10.1080/09638280701654542.

[32] Orendurff MS, Raschke SU, Winder L, Moe D, Boone DA, Kobayashi T. Functional level assessment of individuals with transtibial limb loss: Evaluation in the clinical setting versus objective community ambulatory activity. J Rehabil Assist Technol Eng 2016;3:2055668316636316. https://doi.org/10.1177/2055668316636316.

[33] Gailey RS. Predictive Outcome Measures Versus Functional Outcome Measures in the Lower Limb Amputee. JPO: Journal of Prosthetics and Orthotics 2006;18:P51.

[34] Deathe AB, Wolfe DL, Devlin M, Hebert JS, Miller WC, Pallaveshi L. Selection of outcome measures in lower extremity amputation rehabilitation: ICF activities. Disabil Rehabil 2009;31:1455–73. https://doi.org/10.1080/09638280802639491.

[35] Stepien JM, Cavenett S, Taylor L, Crotty M. Activity levels among lower-limb amputees: self-report versus step activity monitor. Arch Phys Med Rehabil 2007;88:896–900. https://doi.org/10.1016/j.apmr.2007.03.016.

[36] Kim J, Colabianchi N, Wensman J, Gates DH. Wearable Sensors Quantify Mobility in People With Lower Limb Amputation During Daily Life. IEEE Trans Neural Syst Rehabil Eng 2020;28:1282–91. https://doi.org/10.1109/TNSRE.2020.2990824.

[37] John S, Orlowski K, Mrkor K-U, Edelmann-Nusser J, Witte K. Differences in hip muscle strength and static balance in patients with transfemoral amputations classified at different k-levels: a preliminary cross-sectional study. Can Prosthet Orthot J 2022;5. https://doi.org/10.33137/cpoj.v5i1.37456.

[38] John S, Weizel D, Orlowski K, Mrkor K-U, Edelmann-Nusser J, Witte K. Bestimmung von Kraft, Beweglichkeit und Gleichgewicht nach Amputationen der unteren Extremität – Vorstellung eines neuartigen Diagnostikgeräts. Verlag Orthopädie-Technik 2020. https://360-ot.de/bestimmung-von-kraft-beweglichkeit-und-gleichgewicht-nach-amputationen-der-unteren-extremitaet-vorstellung-eines-neuartigen-diagnostikgeraets/ (accessed January 9, 2024).

[39] Orlowski K, Eckardt F, Nusser JE, Witte K. Feedback system for physiotherapy and popular athletes. International Journal of Physiotherapy 2018;5. https://doi.org/10.15621/ijphy/2018/v5i6/178057.

[40] Orlowski K, Eckardt F, Herold F, Aye N, Edelmann-Nusser J, Witte K. Examination of the reliability of an inertial sensor-based gait analysis system. Biomedical Engineering / Biomedizinische Technik 2017;62:615–22. https://doi.org/10.1515/bmt-2016-0067.

[41] Orlowski K, Mrkor K-U, Loose H, John S, Witte K. Investigating the Gait of Lower Limb Amputees Regarding the Present Classification of Mobility Grades: Proceedings of the 13th International Joint Conference on Biomedical Engineering Systems and Technologies, Valletta, Malta: SCITEPRESS - Science and Technology Publications; 2020, p. 336–41. https://doi.org/10.5220/0009175703360341.

[42] Orlowski K, Loose H, Eckardt F, Edelmann-Nusser J, Witte K. Evaluation of Gait Parameters Determined by InvestiGAIT against a Reference System. Proceedings of the 9th International Joint Conference on Biomedical Engineering Systems and Technologies, Rome, Italy: SCITEPRESS - Science and and Technology Publications; 2016, p. 256–62. https://doi.org/10.5220/0005783502560262.

[43] Klute GK, Berge JS, Orendurff MS, Williams RM, Czerniecki JM. Prosthetic intervention effects on activity of lower-extremity amputees. Arch Phys Med Rehabil 2006;87:717–22. https://doi.org/10.1016/j.apmr.2006.02.007.

[44] Arch (Schrank) E, Erol O, Bortz C, Madden C, Galbraith M, Rossi A, et al. Method to Quantify Cadence Variability of Individuals with Lower-Limb Amputation. Journal of Prosthetics and Orthotics 2017;29:1. https://doi.org/10.1097/JPO.0000000000000124.

[45] Zywicki DJ. Advanced signal processing methods applied to engineering analysis of seismic surface waves - ProQuest. Georgia Institute of Technology ProQuest Dissertations Publishing, 1999.

[46] Benedetto JJ, Li S. The Theory of Multiresolution Analysis Frames and Applications to Filter Banks. Applied and Computational Harmonic Analysis 1998;5:389–427. https://doi.org/10.1006/acha.1997.0237.

[47] Krumpholz M, Katehi LPB. MRTD: new time-domain schemes based on multiresolution analysis. IEEE Transactions on Microwave Theory and Techniques 1996;44:555–71. https://doi.org/10.1109/22.491023.

[48] Andén J, Mallat S. Deep Scattering Spectrum. IEEE Trans Signal Process 2014;62:4114–28. https://doi.org/10.1109/TSP.2014.2326991.

[49] Nsugbe E. Particle size distribution estimation of a powder agglomeration process using acoustic emissions. Thesis. 2017.

[50] Nsugbe E, Williams Samuel O, Asogbon MG, Li G. Contrast of multi-resolution analysis approach to trans-humeral phantom motion decoding. CAAI Transactions on Intelligence Technology 2021;6:360–75. https://doi.org/10.1049/cit2.12039.

[51] LeCun Y, Bengio Y, Hinton G. Deep learning. Nature 2015;521:436–44. https://doi.org/10.1038/nature14539.

[52] Bengio Y, Courville A, Vincent P. Representation Learning: A Review and New Perspectives 2014.

[53] Nsugbe E, Obajemu O, Samuel OW, Sanusi I. Application of noninvasive magnetomyography in labour imminency prediction for term and preterm pregnancies and ethnicity specific labour prediction. Machine Learning with Applications 2021;5:100066. https://doi.org/10.1016/j.mlwa.2021.100066.

[54] Nsugbe E, Al-Timemy AH. Shoulder girdle recognition using electrophysiological and low frequency anatomical contraction signals for prosthesis control. CAAI Transactions on Intelligence Technology 2021;n/a. https://doi.org/10.1049/cit2.12058.

[55] Nsugbe E, Starr A, Jennions I, Ruiz-Carcel C. Estimation of online particle size distribution of a particle mixture in free fall with acoustic emission. Particulate Science and Technology 2019;37:953–63. https://doi.org/10.1080/02726351.2018.1473540.

[56] Nsugbe E, Ser H-L, Ong H-F, Ming LC, Goh K-W, Goh B-H, et al. On an affordable approach towards the diagnosis and care for prostate cancer patients using urine, FTIR and prediction machines. Diagnostics 2022;12:2099. https://doi.org/10.3390/diagnostics12092099.

[57] Nsugbe E. On the Application of Metaheuristics and Deep Wavelet Scattering Decompositions for the Prediction of Adolescent Psychosis Using EEG Brain Wave Signals. Digital Technologies Research and Applications 2022;1:9–24. https://doi.org/10.54963/dtra.v1i2.40.

[58] Nsugbe E, Starr A, Ruiz-Carcel C. Monitoring the particle size distribution of a powder mixing process with acoustic emissions: A review. Eng Technol Ref 2016:1–12.

[59] Nsugbe E, Obajemu O, Samuel OW, Sanusi I. Enhancing care strategies for preterm pregnancies by using a prediction machine to aid clinical care decisions. Machine Learning with Applications 2021;6:100110.

[60] Nsugbe E, Connelly S. Multiscale depth of anaesthesia prediction for surgery using frontal cortex electroencephalography. Healthcare Technology Letters 2022;9:43–53. https://doi.org/10.1049/htl2.12025.

[61] Wavelet Scattering. MathWorks n.d. https://uk.mathworks.com/help/wavelet/ug/wavelet-scattering.html.

[62] Mallat S. Group Invariant Scattering. Communications on Pure and Applied Mathematics 2012;65:1331–98. https://doi.org/10.1002/cpa.21413.

[63] Bruna J, Mallat S. Invariant Scattering Convolution Networks. IEEE Trans Pattern Anal Mach Intell 2013;35:1872–86. https://doi.org/10.1109/TPAMI.2012.230.

[64] Liu Z, Yao G, Zhang Q, Zhang J, Zeng X. Wavelet Scattering Transform for ECG Beat Classification. Computational and Mathematical Methods in Medicine 2020;2020:e3215681. https://doi.org/10.1155/2020/3215681.

[65] Nsugbe E, Samuel OW, Asogbon MG, Li G. Phantom motion intent decoding for transhumeral prosthesis control with fused neuromuscular and brain wave signals. IET Cyber-Systems and Robotics 2021;3:77–88. https://doi.org/10.1049/csy2.12009.

[66] Charbuty B, Abdulazeez A. Classification Based on Decision Tree Algorithm for Machine Learning. Journal of Applied Science and Technology Trends 2021;2:20–8. https://doi.org/10.38094/jastt20165.

[67] Klecka WR, Iversen GR, Klecka WR. Discriminant Analysis. SAGE; 1980.

[68] LaValley MP. Logistic regression. Circulation 2008;117:2395–9. https://doi.org/10.1161/CIRCULATIONAHA.106.682658.

[69] Kramer O. K-Nearest Neighbors. Dimensionality Reduction with Unsupervised Nearest Neighbors, vol. 51, Berlin, Heidelberg: Springer Berlin Heidelberg; 2013, p. 13–23. https://doi.org/10.1007/978-3-642-38652-7_2.

[70] Rosenbaum DA. Human Motor Control. Academic Press; 2009.

[71] Schott GD. Penfield's homunculus: a note on cerebral cartography. J Neurol Neurosurg Psychiatry 1993;56:329–33.

[72] Kooijman CM, Dijkstra PU, Geertzen JHB, Elzinga A, van der Schans CP. Phantom pain and phantom sensations in upper limb amputees: an epidemiological study. Pain 2000;87:33–41. https://doi.org/10.1016/S0304-3959(00)00264-5.